IAC-13,A6,2,3x19121

A SIMPLIFIED APPROACH TO ANALYZE THE SPACE DEBRIS EVOLUTION IN THE LOW EARTH ORBIT

Christopher Kebschull[a], V. Braun[a], S. Flegel[a], B. Reihs[a], S. Hesselbach[a], J. Gelhaus[a], M. Möckel[a], J. Radtke[a], C. Wiedemann[a], H. Krag[b], P. Vörsmann[a]

[a] *Institute of Aerospace Systems, Technische Universität Braunschweig, Hermann-Blenk-Str. 23, 38108 Braunschweig, Germany*
[b] *Space Debris Office, ESA/ESOC, Robert-Bosch-Str. 5, 64293 Darmstadt, Germany*

Abstract

During the past 60 years the number of objects on Earth orbits has increased. So has the risk of collisions, which is likely to be the main driver for space debris generation in the future. This is important, for example, in densely populated regions like the sun-synchronous orbit at around 800 km altitude. In order to predict the future development of the debris environment numerical simulations can be used. These simulations are usually based on initial assumptions like the launch rate, the probability distribution of success of post mission disposal measures and the likelihood for catastrophic collisions. The computationally expensive Monte-Carlo method is employed for the random sampling of the defined events. Additionally, a propagator needs to process the objects to determine potential collision partners, increasing the demand for computing power even further. In this paper an analytical model is presented, which is based on source and sink mechanisms, like launches, collisions and explosions. In this approach different altitude shells and diameter bins, as well as four different object classes for intact objects and fragments, each on circular and eccentric orbits are considered. By using pre-computed tables for orbital lifetimes and decay rates, both the computational effort and complexity of the model are decreased. The model can be adjusted to reflect different forecasts by altering the decay and collision rates. The paper concludes by showing preliminary results and a discussion of the generic approach, which allows the model to be fitted against more computationally expensive Monte-Carlo simulations.

Keywords: Analytical model, Evolution, Space debris

I INTRODUCTION

The simulation of the evolution of the future space debris population is often performed by means of numerical computations. They account for all effects which have a considerable impact on that population. Often, these simulations involve the computation of orbits as well as the evaluation of potential fragmentation events for more than 100,000 objects. In order to have a statistical significance Monte-Carlo runs have to be performed as many events are triggered randomly according to a defined probability distribution. In order to avoid the enormous computational demand of those numerical methods, an analytical model is being developed, considering all the relevant effects in LEO through source and sink mechanisms and representing them as differential equations. These equations are solved by a simple Euler integrator to provide the evolution of the space debris population for any arbitrary instant in time. In order to keep the complexity of the model and the computational demand low, a number of altitude shells are used to describe the LEO region in the range of 300 to 2.000 km. Intact objects and fragments are also grouped into diameter classes starting from 10 cm to 100 m. Similar approaches have been explored in [1] and [2]. However, in this new model more source and sink mechanisms are considered as well as extra eccentricity classes. The NASA breakup model is used to estimate the rate of fragments caused by collisions and explosions [3]. The formulation of the equations is kept generic in the sense that the user of the implementation can decide how many shells and classes are to be used in the simulation. A partial implementation of the model could be used to pro-

Email address: c.kebschull@tu-braunschweig.de (Christopher Kebschull)

duce preliminary results, as shown in Sec. III. In this paper results from the numerical tool LUCA (Long-Term Utility for Collision Analysis) have been used to fit the parameters of the differential equations.

II THE MODEL

The analytical model is valid for the complete LEO region, which is defined here from 300 to 2,000 km altitude. This is due to the assumption that objects below 300 km in any case will not have an orbital lifetime that would significantly contribute to the long-term evolution of the space debris environment. The LEO region is subdivided into altitude shells h_i. The object classes are further subdivided into diameter classes d_i, perigee radius classes $r_{p,i}$ and eccentricity classes ε_i. The perigee and eccentricity classes are used for eccentric orbits only. An orbit is considered to be eccentric if the difference between perigee and apogee altitude is greater than the defined altitude shell, i.e. the object would pass through multiple altitude shells. If an object is eccentric, it is equally distributed with respect to the altitude shells it passes. At each instant of time the number of objects for a given altitude shell h_i, a diameter class d_i and (for eccentric orbits) for perigee and eccentricity classes $r_{p,i}$ and ε_i respectively, is given via:

$$\begin{aligned} N &= f(d_i, h_i, r_p, \varepsilon, t) \\ &= N_{I_c} + N_{I_e} + N_{F_c} + N_{F_e}, \end{aligned} \tag{1}$$

where intact bodies N_I and fragments N_F are treated separately. Each object is defined through its diameter class d_i, altitude shell h_i and for objects on eccentric orbits their perigee altitude $r_{p,i}$ and eccentricity ε. The change over time of the number of objects in a given altitude shell is expressed through a set of differential equations:

$$\dot{N} = \frac{dN}{dt} = \frac{dN_{I_c}}{dt} + \frac{dN_{I_e}}{dt} + \frac{dN_{F_c}}{dt} + \frac{dN_{F_e}}{dt}, \tag{2}$$

which are then used to analytically determine the number of objects as a function of time using Euler's method:

$$N = N_0 + \dot{N} \cdot \Delta t. \tag{3}$$

As the number of initial objects N_0 the MASTER-2009 reference population is used. The integration interval Δt is assumed to be one year. In the following the source and sink mechanisms for intact bodies are described. Fig. I shows the basic principle of this model. For a given altitude shell h_i the source for gaining objects and sink for losing objects is the natural decay which can enter the shell from higher altitudes respectively leave the shell to a lower one. A launch rate L is a source that takes into account that new objects are added to the various altitude shells. In this paper a sequence of launches

Nomenclature

Latin symbols:

A	cross-sectional area
ADR	rate of actively removed objects
E	kinetic energy
FRG	fragment creation rate
H	scale height
L	launch rate
M	molar mass
MRO	mission related object rate
N	number of objects
$\dot{N}$	rate of objects
$\bar{N}$	discrete rate of objects
PMD	post mission disposal rate
R	ideal gas constant
T	temperature
c	scaling/fitting parameter
d	diameter
f	function
h	altitude
m	mass
n	maximum number of classes/shells
p	probability
r	radius
v	velocity

Greek symbols:

β	correction factor
Δt	time step
γ	fitting parameter
ε	eccentricity
μ	standard gravitational parameter
ρ	density
σ	average cross-section
τ	residence time

Indices:

I	intact objects
F	fragments
c	circular orbit
col	collision
e	eccentric orbit
exp	explosion
i	interval index
im	impact
$i+$	upper interval bound
$i-$	lower interval bound
k	first diameter class index
l	second diameter class index
p	perigee
pr	projectile
q, r, s, t	shell/class indices

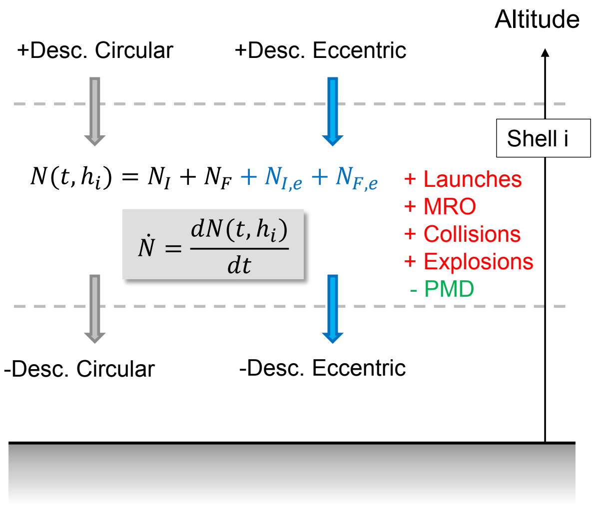

Fig. I: The source and sink mechanism.

is defined over an eight year time span. This value is based on the assumption of an average mission duration of eight years after which a satellite is at the end of its life and has to be replaced. At the end of a mission the payload can be removed from a given altitude shell through post mission disposal (PMD) maneuvers, for example to be in line with the Space Debris Mitigation Guidelines (SDMG) [4]. Within the scope of the PMD-sink can also be a time delayed active debris removal mission (ADR). During a launch, mission related objects (MROs) can be released. As the payloads and rocket bodies they also appear in the altitude shells following the previously described sequence. Based on their area-to-mass ratio however they are counted to the fragment population in this model. The two sources of fragments are explosion and collision events. While in numerical simulations they are triggered individually based on a random variable in this model they are treated as a source of fragments which are continuously generated. Also the fragment generation process is confined to the orbit at which it is generated. This means that neither a collision nor an explosion can spread fragments over multiple altitude shells. The only sink for fragments is the natural decay. In the following the differential equations are introduced. Note that some of them have two definitions, one for objects on circular orbits and one for eccentric orbits. Also intact bodies and fragments are distinguished.

II.1. Intact bodies

For intact bodies the following differential equation is used to express the rate at which the number of objects changes in a given time step t:

$$\dot{N}_I = \frac{dN_I}{dt} = L + \bar{N}_{I_c} + \bar{N}_{I_e} \\ - ADR - PMD - \bar{N}_{I_{col}} - \bar{N}_{I_{exp}}, \quad (4)$$

where L is the launch rate, ADR the rate of actively removed objects and PMD the rate of objects removed through post mission disposal. Each are given as rates in yrs^{-1}. $\bar{N}_c$ and $\bar{N}_e$ are the rates at which circular and eccentric bodies are passing through a given altitude shell h_i due to drag. Objects which are involved in a fragment generation event ($\bar{N}_{I_{col}}$ and $\bar{N}_{I_{exp}}$) are removed from the intact body list.

II.1.1. Launches

The launch rate is given through a predefined sequence of intact objects that are injected into the LEO over a time period of one year. Based on a typical mission duration an eight year repeating sequence is used in this paper. So the launch rate depends only on the time t:

$$L = f(t). \quad (5)$$

Launches are the source of creating new intact bodies. The launch rate has to provide the diameter and altitude (for circular orbits) or perigee radius and eccentricity (for eccentric orbits) for each object. It is provided as a lookup table.

II.1.2. Natural Decay

The only natural sink in the model is the decay caused through the drag in the residual atmosphere. For intact bodies and fragments the relation is given in equations 6 and 7:

$$\bar{N}_c = \frac{N_c}{dt} = \frac{N_c(d_i, h_{i+1})}{\tau_c(d_i, h_{i+1})} - \frac{N_c(d_i, h_i)}{\tau_c(d_i, h_i)}. \quad (6)$$

The rate at which the objects are passing through the altitude shell is defined by the number of objects entering the shell from higher altitudes and the ones decaying to lower altitudes in the given timeframe τ. It is valid only for the given altitude shell. It describes the average residence time in that shell.

$$\bar{N}_e = \frac{N_e}{dt} = \frac{N_e(d_i, h_{i+1}, r_p, \varepsilon)}{\tau_e(d_i, h_{i+1}, r_p, \varepsilon)} - \frac{N_e(d_i, h_i, r_p, \varepsilon)}{\tau_e(d_i, h_i, r_p, \varepsilon)} \quad (7)$$

The residence time in altitude shells for circular orbits is described through τ_c:

$$\tau_{I_c} = f(d_i, h_i, A/m_I). \quad (8)$$

with a conservative estimate for the area-to-mass ratio for intact objects which has been set to:

$$\left(\frac{A}{m}\right)_I = c_I \cdot 0.005\ m^2/kg. \quad (9)$$

This number represents 70% of payloads and rocket bodies on the priority list, which have been generated at the ILR [5] in a previous study. The coefficient c_I is used to fit the decay rate of the intact objects to achieve a more realistic value. This approach can be further extended by using different ratios per diameter bin (d_i).
Based on the residence time for circular orbits τ_c is the residence time in altitude shells for eccentric orbits:

$$\tau_{I_e} = \tau_{I_c} \cdot f(\varepsilon, h_i), \tag{10}$$

where $f(\varepsilon, r_p)$ is a correction factor determining the residence times of eccentric orbits in their more than one altitude shell spanning orbit. An object on each eccentric orbit will spend a fraction of the time in the altitude shells it is crossing. So τ_e will determine the fraction for a given orbit. In the interpretation from the point of view of the model a fraction of the object is considered in all altitude shells its trajectory is crossing. For example, an object having its perigee at altitude shell h_i and its apogee at altitude shell h_{i+2} would be represented as 1/3 objects in h_i, 1/3 in h_{i+1} and 1/3 in h_{i+2}. The object would be distributed equally among the altitude shells. The object fraction is determined as 1/n, where n is the number of altitude shells crossed by the object.

II.1.3. Active debris removal and post mission disposal

Due to active debris removal (ADR) it is possible to remove a given number of intact objects per year from an altitude shell:

$$ADR = f(d_i, h_i). \tag{11}$$

A second factor which speeds up removal of objects from altitude shells is the deployment of post mission disposal measures. It comprises the 25 year rule as stated in the SDMG [4] in this model:

$$PMD = f_s \cdot L(d_i, h_i). \tag{12}$$

The PMD rate is based on the previous launch sequence and thus on the launch rate. The success rate of a PMD maneuver can be influenced by the parameter f_s, which can be defined in the input of the model. When a PMD was successfully executed (f_s) the given object is transferred from the a circular orbit into an eccentric one, where its residual lifetime on orbit is 25 years.

II.2. Fragments

For fragments the differential equation is defined as follows:

$$\dot{N}_F = \frac{dN_F}{dt} = \bar{N}_{F_c} + \bar{N}_{F_e} + FRG_{col} + FRG_{exp} + MRO. \tag{13}$$

The fragments on circular ($\bar{N}_{F_c}$) and eccentric orbits ($\bar{N}_{F_e}$) follow the same relation as stated in equations 6 and 7. However for fragments a different area-to-mass ratio is assumed:

$$\left(\frac{A}{m}\right)_F = c_F \cdot 0.12\ m^2/kg. \tag{14}$$

The factor c_F is a coefficient which is later being used to fit the decay rate of fragments for the model.

II.2.1. Collision fragments

Collision fragments are created through collisions of two objects, which can be intact objects and fragments on circular orbits. Each diameter class (d_k) is paired with another class (d_l). Each of them can create fragments that are smaller than the classes themselves. However, due to the nature of a fragmentation those involved objects break up into a wide range of different sized fragments. These then have to be correlated with the correct diameter class (d_i) in which they are held to compute the correct fragment generation rate. This is done for each altitude shell. In our assumption fragments generated from objects on circular orbits are generated to stay in the same orbital region wrt. classes and do not build up an eccentricity, thus do not spread across different altitude shells:

$$FRG_{col}^{cc} = \sum_{k=1}^{n_d} \sum_{l \le k}^{n_d} f_{col}(d_l, d_i) \cdot p(h_i, t, N) \cdot \sigma(d_k, d_l) \cdot N(d_k, h_i) \cdot N(d_l, h_i). \tag{15}$$

The chance of generating fragments is expressed through the probability $p(h_i, t, N)$. Based on the MASTER-2009 population a probability relation as a function of N has been derived, where the number of objects in an altitude shell (h_i) correlates directly with the probability of a collision:

$$p(h_i, N(h_i)) = \alpha_0(h_i) + \alpha_1(h_i) \cdot N(h_i). \tag{16}$$

The coefficients α_0 and α_1 have been preprocessed and are available using a lookup table. The σ in the equation above is defined as:

$$\sigma(d_k, d_l) = \frac{1}{4} \cdot (d_k + d_l)^2\,. \tag{17}$$

It is the combined cross-section of the two objects defined with the diameters d_l and d_k. Eq. 18 defines the amount of fragments that is generated. In conjunction with c_{col} it is downscaled so that it can be seen as a fragmentation rate for a given time interval rather than an absolute number of created fragments:

$$f_{col}(d_l, d_i) = \sum_{i=1}^{d_l} c_{col} \cdot \left(N^*_{F,col}(d_{i-}) - N^*_{F,col}(d_{i+})\right). \tag{18}$$

$N^*_{F,col}$ represents the number of fragments generated when an object of a given diameter is being fragmented. For a fragmentation all diameter classes including the largest one defined as d_l are updated (hence the sum). The generation of fragments is defined through a power law in the NASA breakup model [3]:

$$N^*_{F,col}(d) = 0.1 \cdot \hat{m}_e^{0.75} \cdot \hat{d}^{-1.71}, \tag{19}$$

where $\hat{d}$ is a normalized object parameter:

$$\hat{d} = \frac{d}{1\,m}, \tag{20}$$

and $\hat{m}_e$ is defined as:

$$\hat{m}_e = \begin{cases} \dfrac{m_{sat} + m_{pr}}{1\,kg} & \forall \tilde{E}_{pr} \geq \tilde{E}^*_{pr} \\ \dfrac{m_{pr} \cdot v_{im}}{1000\,\frac{kgm}{s}} & \forall \tilde{E}_{pr} < \tilde{E}^*_{pr} \end{cases} \tag{21}$$
$$\tilde{E}_{pr} = \frac{m_{pr} \cdot v_{im}^2}{2 \cdot m_{sat}}\ , \quad \tilde{E}^*_{pr} = 40\ J/g,$$

with m_{sat} being the mass of the parent object (kg), m_{pr} the mass of the projectile (kg), $v_{I'm}$ the impact velocity (km/s), $\tilde{E}_{pr}$ the specific kinetic energy of the projectile (J/g) and $\tilde{E}^*_{pr}$ the critical specific Energy (J/g). In the context of the analytical model, the terms parent and projectile are not distinguished, e.g. by assuming that projectiles have a significantly lower mass than the parent. Furthermore, even collisions between objects of the same size are paired and the same relation of the NASA breakup model is applied. Eq. 22 and 23 describe the pairing of objects on circular and eccentric respectively eccentric and eccentric orbits:

$$FRG^{ec}_{col} = \sum_{k=1}^{n_d} \sum_{l \leq k}^{n_d} \sum_{q=1}^{n_{rp}} \sum_{r=1}^{n_\varepsilon} f_{col}(d_k, d_l, d_i) \cdot p(h_i, t, N) \cdot \sigma(d_k, d_l) \cdot N(d_k, h_i, r_{p,q}, \varepsilon_r) \cdot N(d_l, h_i), \tag{22}$$

$$FRG^{ee}_{col} = \sum_{k=1}^{n_d} \sum_{l \leq k}^{n_d} \sum_{q=1}^{n_{rp}} \sum_{r=1}^{n_\varepsilon} \sum_{s=1}^{n_{rp}} \sum_{t=1}^{n_\varepsilon} f_{col}(d_k, d_l, d_i) \cdot p(h_i, t, N) \cdot \sigma(d_k, d_l) \cdot N(d_k, h_i, r_{p,q}, \varepsilon_r) \cdot N(d_k, h_i, r_{p,s}, \varepsilon_t). \tag{23}$$

II.2.2. Explosion fragments

Fragments due to explosions can occur only for intact bodies (N_I):

$$FRG_{exp} = f_{exp}(d_i) \cdot p_{exp}(t) \cdot N_I(d_i, h_i). \tag{24}$$

The probability p_{exp} expresses the chance of an explosion event to occur. In the model this can be defined as an input parameter. The amount of generated explosion fragments in a defined diameter class is defined as:

$$f_{exp}(d_i) = c_{exp} \cdot \left(N^*_{F,exp}(d_{i-}) - N^*_{F,exp}(d_{i+})\right), \tag{25}$$

where d_{i-} is the lower interval border and d_{i+} is the upper interval border. In this expression fragments, are generated for the specified interval. In order to be able to fit these results later, on the scaling parameter c_{exp} is introduced. It will enable to scale the generated amount of fragments down, so it can be considered being a fragment rate rather than an absolute number of fragments. The NASA breakup model is also being used for the generation of the explosion fragments:

$$N^*_{F,exp}(d) = 6 \cdot s \cdot \hat{d}^{-1.6}. \tag{26}$$

An amount of explosion fragments $N^*_{F,exp}$ larger than $\hat{d}$, as defined in Eq. 20 is created. The scaling factor s is a function of the parent object. In the analytical model, the scaling factor is assumed to have a value of 1.0 in order to be conservative, while especially for many russian rocket bodies this value may be significantly lower.

II.2.3. Mission related objects

MRO is the rate at which new mission related objects are created in a given altitude shell. In this model MROs are directly linked to the launches L. However due to their higher area-to-mass ratio they are considered as fragments:

$$MRO = f(L). \tag{27}$$

III PRELIMINARY RESULTS

The described model has been implemented in FORTRAN. To make sure the chosen approach is valid each source and sink component is compared individually against the LUCA model. In the current state of development only objects on circular orbits are considered. Also the ADR and PMD components as well as the explosion fragments are currently under development.

III.1. Launch traffic and initial population

For the launch rate $L(t)$ a launch pattern adding 31 to 42 new objects per year into the given altitude and diameter classes is assumed. With an average mission duration of eight years this pattern is being repeated, as shown in Fig. II. Based on the MASTER model an initial population N_0 is used to the reference epoch May 1st, 2009. Fig. III shows the initial population within the 34 defined altitude shells used as a starting point for the simulation. Fig. IV shows the initial population within the 12 diameter classes. The lower limit has been set

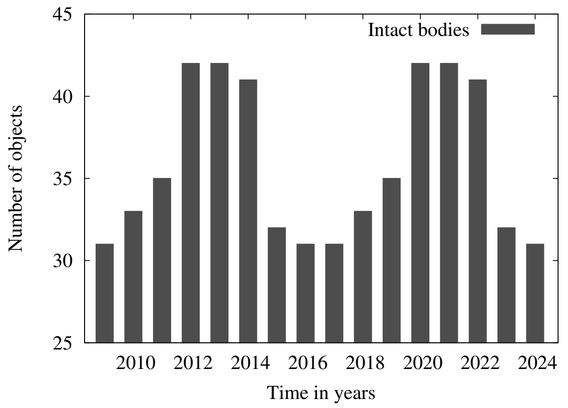

Fig. II: The launch traffic which is repeating every eight years.

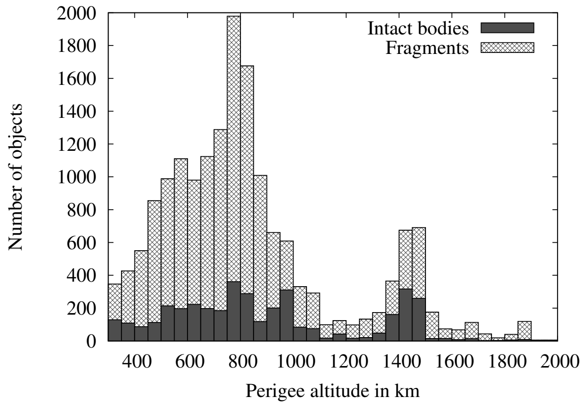

Fig. III: The initial population as number of objects over the perigee altitude.

to 10 cm, while the upper bound is 100 m. A logarithmic approach has been chosen to distribute the objects among the classes. Eq. 28 has been used to determine the upper bound of each class.

$$d(i) = 10^{(0.25 \cdot i - 1)}. \tag{28}$$

III.2. Launches and natural decay

The natural decay for objects on circular orbits has been described in Eq. 6. It estimates how many objects are passing through an altitude shell based on their residence time (Eq. 8) in the given shell and the shell above. The residence time is primarily influenced by the drag force in LEO. In the current implementation the relation in Eq. 29 is being used to retrieve the residence time.

$$t_d(h_i, d_i) = \frac{B \cdot H}{\sqrt{\mu_E \cdot h_{i-}} \cdot \rho_0} \cdot (1 - \mathrm{e}^{-\frac{h_{i+} - h_{i-}}{H}}) \tag{29}$$

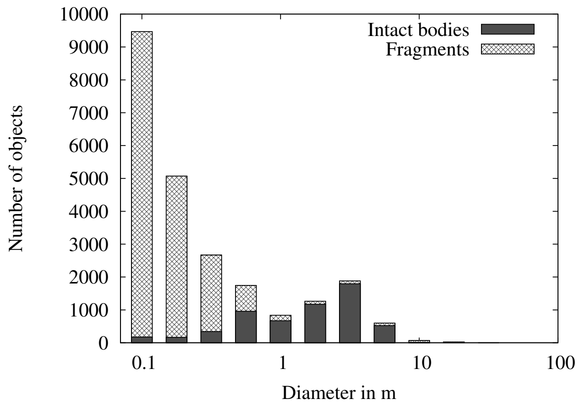

Fig. IV: The initial population as number of objects over the diameter.

The altitude shell's lower and upper bounds, h_{i-} respectively h_{i+}, as well as the standard gravitational parameter μ_E are needed. The density of the atmosphere ρ_0 is supplied by the atmospheric model. The ballistic coefficient B uses the given area-to-mass (A/m) ratio and a fixed value of 2.2 for the coefficient of drag c_D:

$$B = \frac{m}{c_D \cdot A}. \tag{30}$$

The scale height H also relies on the atmospheric model, where T and M are the temperature and molar mass of the surrounding atmosphere and the ideal gas constant R.

$$H = \frac{r^2 \cdot R \cdot T}{\mu \cdot M} \tag{31}$$

The atmosphere is currently being modeled using an approach by Jacchia as described in [6]. Based on the two sources *launches* and *natural decay* Fig. V shows the evolution of the intact bodies over time. The LUCA model shows a periodic fluctuation based on the influence of solar and geomagnetic activity. The analytical model (AM) slightly overestimates the results by LUCA and also shows a minor fluctuation over a period of eight years. This is based on the launch pattern mentioned previously. The launch pattern is identical to the one used in LUCA. However in the LUCA results they are superimposed by the effect the solar and geomagnetic activity has on objects in LEO. Fig. VI shows the evolution of the fragments over time. The initial results produced by the analytical model using c_F=1 for the fitting parameter, deviate quite strongly from LUCA's numerical approach. For this reason the fitting parameter has been varied. A value of $c_F = 0.3$ has turned out represent LUCA's results well. It is also recognizable that the LUCA model reflects the periodic nature of the solar activity in the fluctuating increase and decrease of the decay rate, while

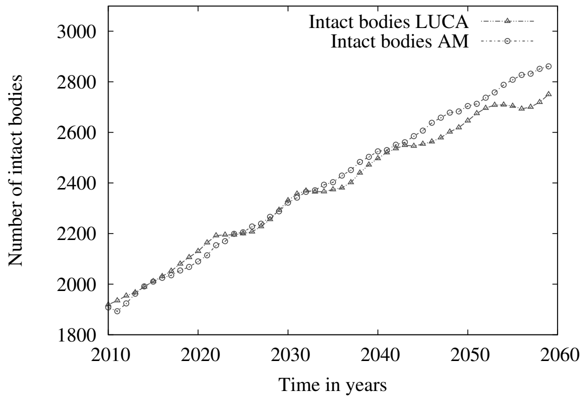

Fig. V: The evolution of the intact bodies over time as produced by LUCA and the AM.

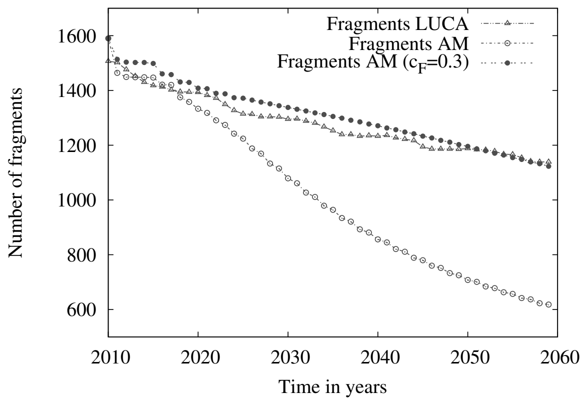

Fig. VI: The evolution of the fragments over time as produced by LUCA and the analytical model (AM).

the analytical model does not. This is due to the previous stated fact that the current version of the analytical model uses a constant solar activity setting. After looking separately at the evolution of the intact bodies and fragments over time, the number of all objects over the 34 altitude shells for different points in time will now be analyzed. Fig. VII shows the prediction for the year 2035. It is visible that the analytical model follows the trend over the altitude shells as predicted by LUCA. In most orbits the differences are very low with a median variation of 9.3 %. However in the 750 km and 800 km bins the analytical model shows the largest absolute variations. While the 750 km altitude shell is underestimated by 90.2 objects, the 800 km shell is overestimated by 105.9 objects. On the other hand the 350 km and the 1550 km shells show the biggest relative variations, with a discrepancy of 93.33 % and 132.5 %. These outliers

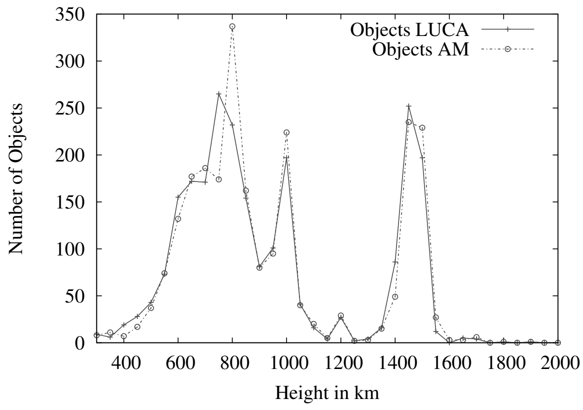

Fig. VII: The evolution of the objects over the altitude for the year 2035 as produced by LUCA and the analytical model (AM).

are caused by low object counts within the considered altitude shells, which means that small absolute variations already produce considerable relative differences. When predicting even further into the year 2059 the analytical model is also able to follow the trend which is anticipated by LUCA. In comparison to the previous consideration the median variation between the two models however goes up to 13.61 %. While the 750 km altitude shell is now almost inline with LUCA's prediction the lower altitude shells show more variations than before with differences of up to 63.4 objects per shell. The 800 km altitude shell is still overestimated with 108.9 % objects more than LUCA's model predicts. As before the altitude shells at 350 km and 1550 km show the biggest relative variations of over 100 %. Again this is caused by the low object count within the considered altitude shells.

III.3. Collision fragments

The generation of collision fragments for circular orbits is introduced with Eq. 15, which generates a continuous amount of fragments based on the diameter and altitude shells as well as a probability relation. In the current state of implementation the probability relation p has not been finalized yet. For the following results each altitude shell uses the relation which is valid for the 800 km altitude. It has the highest collision probability of all altitudes. Thus the fragment generation rate in almost all other shells is overestimated, as shown in Fig. IX. At this point however it is already recognizable that the trend can be described by the chosen approach. Fig. X shows the amount of generated fragments over the diameter for the 800 km altitude shell. It is recognizable that the analytical model underestimates the fragment rate in this altitude shell. For diameter classes between 1 m and

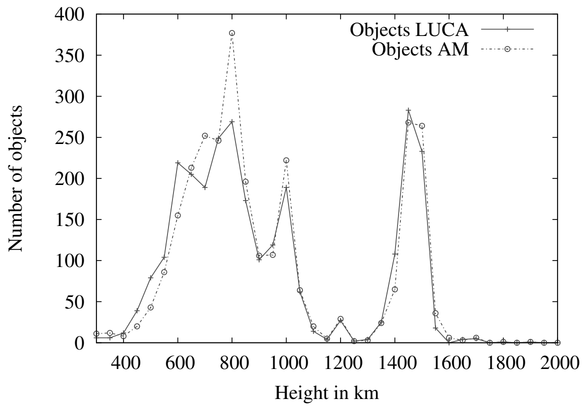

Fig. VIII: The evolution of the objects over the altitude for the year 2059 as produced by LUCA and the analytical model (AM).

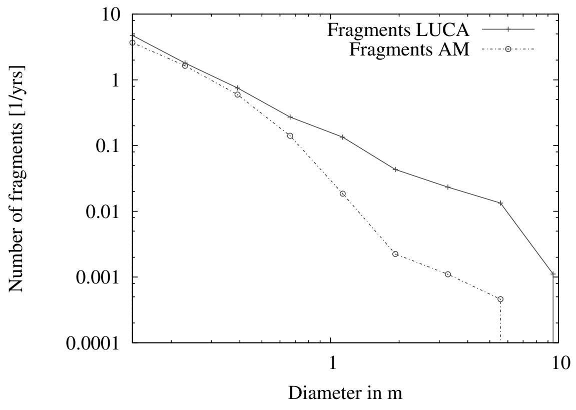

Fig. X: The generation of fragments over the diameter bins within one year for the 800 km altitude shell.

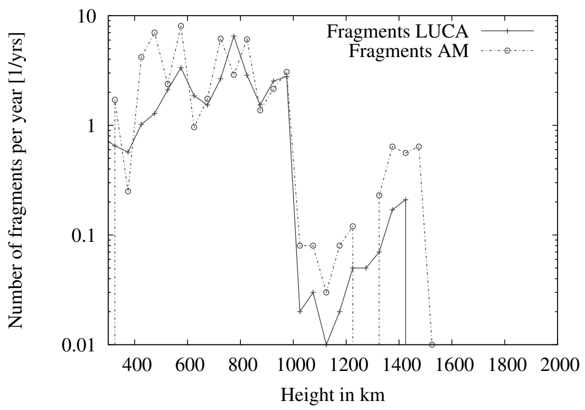

Fig. IX: The generation of fragments over the altitude shells within one year.

$\hat{h}_i$ [-]	β_1 [-]	β_2 [-]
800	-0.965767	4.194000
850	-0.976748	3.810730

Tab. I: Exemplary values for the parameters β_1 and β_2.

10 m the differences deviate quite strongly. However in these classes only minor fractions of fragments are generated. In order to achieve the above results the scaling parameter c_{col} in Eq. 15 has to be adjusted. Without the adjustment the fragment generation rate would be overestimated by order of several magnitudes. The parameter corrects this shortcoming and has been derived using twelve different initial populations. It turns out that a more complex relation is needed:

$$\begin{aligned} c_{col} &= f\left(N(h_i), N(h_i, d_i), \hat{d}_i, \hat{h}_i, \triangle\hat{h}_i\right) \\ &= \gamma\left(\hat{d}_i, \hat{h}_i\right) + \left[\frac{N(h_i, d_i)}{N(h_i)} + \frac{\triangle\hat{h}_i}{\hat{h}_i}\right] \cdot 10^{-3} \end{aligned} \tag{32}$$

where $\hat{d}$ and $\hat{h}$ are normalized values of the diameter respectively the altitude and $\triangle\hat{h}$ is the normalized altitude shell size:

$$\hat{d}_i = \frac{d_i}{1\ m} \tag{33}$$

$$\hat{h}_i = \frac{h_i}{1\ km} \tag{34}$$

$$\triangle\hat{h}_i = \frac{h_{i+} - h_{i-}}{1\ km} \tag{35}$$

The newly introduced parameter γ is a function of the diameter and takes into account that smaller particles are underrepresented in the chosen approach:

$$\gamma\left(\hat{d}_i, \hat{h}_i\right) = \left(\beta_1\left(\hat{h}_i\right) + 1\right) \cdot e^{-\beta_2\left(\hat{h}_i\right)\cdot\hat{d}_i} \tag{36}$$

The correction parameters β_1 and β_2 also reflect an altitude dependence as shown in Fig. XI using the numerically determined values as shown in Tab. I. This method will be simplified in the future once the rest of the model has been implemented and fitted against LUCA.

IV FUTURE WORK

At this point the described equations in Sec. II have been implemented partially so that first results could be produced and a fitting process could be established, as shown in Sec. III. Consequently the next steps are the implementation of the remaining source and sink mechanisms in equations 11, 12, 26 and 27. For the natural

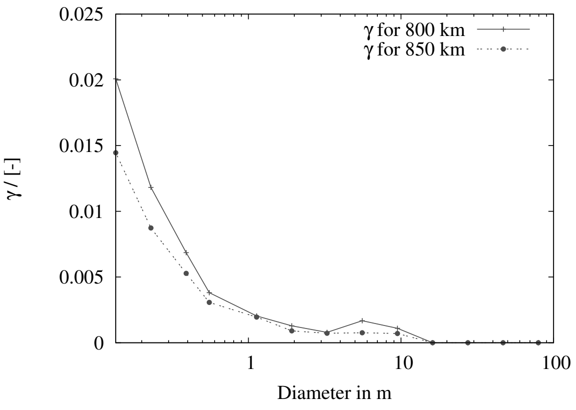

Fig. XI: The distribution of the parameter gamma in dependence on the diameter exemplary for the shells 750-800 km and 800-850 km.

decay sink mechanism the current approach using Jacchia's atmospheric model to determine the drag and thus the residence time of objects in a given altitude shell will be replaced by a lookup table so that the equation, which determines the residence times of eccentric objects (Eq. 10) can be implemented. The lookup table will be based on results that have been produced with ESA's OSCAR tool, which is part of the new DRAMA software suite [7]. Following this step is the consideration of eccentric orbits when generating collision fragments by implementing equations 22 and 23. They pair objects on circular orbits with objects on eccentric orbits and also objects on eccentric orbits with one another. Currently only objects on circular orbits cause the production of fragments. Finally the collision probability p, which is used to describe the altitude dependent chance of a fragmentation event in Eq. 16 will be based on a lookup table so that the parameters α_0 and α_1 can be retrieved for every altitude shell. Currently only the values for the 800 km shell are implemented, leading to an overestimation of collision fragments in the higher and lower altitude shells.

V CONCLUSION

In this paper the mathematical background of an analytical model has been introduced, which is based on previously explored theories by Lewis [1] and Rossi [2]. The equations have been implemented into a software and a fitting process toward the numerical simulation LUCA has been performed. Preliminary results show that the natural decay and fragmentation events for different initial populations are modeled sufficiently by the chosen approach. The next steps include further implementation of the described equations and creating lookup tables for the fragmentation probability and natural decay in the defined altitude shells. One of the main goals to reduce the processing time with this approach as compared to numerical simulations has so far been achieved. The runtime of the software is within the order of seconds as compared to the much more complex, numerical simulation LUCA, which can run hours, or even up to days based on the selected amount of Monte-Carlo runs.

VI ACKNOWLEDGMENTS

The development of the described analytical model is a part of the project *Fragmentation Consequence Analysis for LEO and GEO Orbits* supported by ESA's General Studies Programme (contract 4000106517/12/F/MOS).

VII REFERENCES

[1] H. G. Lewis, G. G. Swinerd, R. J. Newland, and A. Saunders, "The fast debris evolution model," *Advances in Space Research*, vol. 44, pp. 568–578, 2009.
[2] A. Rossi, A. Cordelli, P. Farinella, and L. Anselmo, "Collisional evolution of the earth's orbital debris cloud," *Journal of Geophysical Research*, vol. 99, pp. 23,195–23,210, November 1994.
[3] N. L. Johnson, P. H. Krisko, J.-C. Liou, and P. D. Am-Meador, "Nasa's new breakup model of evolve 4.0," *Advances in Space Research*, vol. 28, no. 9, pp. 1377–1384, 2001.
[4] UN Office for Outer Space Affairs, *Space Debris Mitigation Guidelines of the Committee on the Peaceful Uses of Outer Space*, 2010.
[5] C. Kebschull *et al.*, "Active removal of satellites," tech. rep., ILR/Astrium Gmbh Bremen Study B60/4500160249, 2012.
[6] L. Jacchia, "Thermospheric temperature, density and composition: New models.," *Smithsonian Astrophysical Observatory*, 1977.
[7] J. Gelhaus, N. Sánchez-Ortiz, *et al.*, *DRAMA Final Report – Upgrade of ESA's Space Debris Mitigation Analysis Tool Suite*, 2013.